the attenuation directly over the range 5 to 25 db with an accuracy of ± 0.1 db, which is often useful for rapid measurements. Over this same range the phase change through the instrument is 2 degrees.

For less accurate measurements flap attenuators are used, in which a differential screw motion moves a 2-mil thick metalized mica vane vertically through a 5-mil slot in the waveguide, the top of the slot being surrounded by loaded epoxy resin to eliminate leakage of power from the guide. The RG136 components have an insertion loss of 0.5 db, a range of 20 db and a resetting accuracy of about 0.03 db.

Variable short circuits are of the noncontacting type, with a cylindrical, choked piston moving in precision electroformed waveguide. The movement is through a micrometer screw, calibrated at 0.01-mm intervals. At 140 Gc VSWR's of 25 to 30 are obtained, corresponding to voltage reflection coefficients of 0.92 to 0.94.

For matching purposes a version of the pivoting screw tuner[5] is used, giving a very smooth action. The RG136 device uses an 8-mil diameter probe in a 12-mil wide slot and the RG139 version a 4-mil probe in an 8-mil slot. The slot and the recesses in the top waveguide wall, to allow the saddle holding the probe to pivot and still remain in close contact with the wall, are spark eroded in one operation using a tool as shown in Fig. 8.

[5] C. W. van Es, M. Gevers and F. C. de Ronde, "Waveguide equipment for 2 mm microwaves," *Philips Tech. Rev.*, vol. 22, No. 4, p. 113, No. 6, p. 181; 1960–1961.

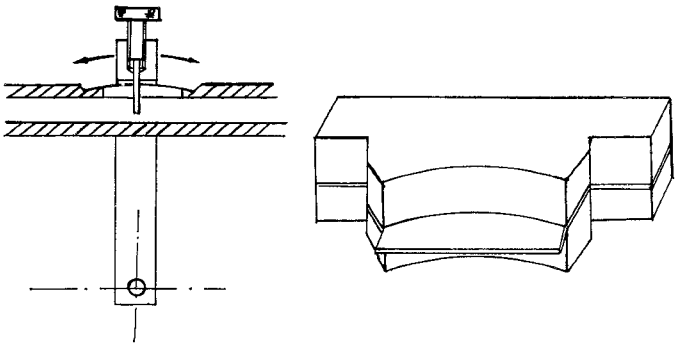

Fig. 8—Tool used in spark eroding a pivoting screw tuner.

Conclusions

Despite the small waveguide sizes and high wall losses it is possible to make useful waveguide components of a conventional type in fundamental mode rectangular guide for a wavelength of 2 mm and, almost certainly, of 1 mm.

Acknowledgment

This work would not have been possible but for the help of the Engineering Department, Royal Radar Establishment, and the aid of our colleagues of the Millimeter Wave Division.

The authors thank the United Kingdom Atomic Energy Authority for supporting this work and the Ministry of Aviation for permission to publish this paper.

Submillimeter Components Using Oversize Quasi-Optical Waveguide*

J. J. TAUB†, SENIOR MEMBER, IEEE, H. J. HINDIN†, MEMBER, IEEE, O. F. HINCKELMANN†, MEMBER, IEEE, AND M. L. WRIGHT†, MEMBER, IEEE

Summary—**Components such as directional couplers, attenuators, and phase shifters have been developed using optical techniques in oversize rectangular waveguide. These components were designed for operation in the 300- to 350-Gc range. They were scaled from a design that was successful at 27 Gc. Preliminary data taken at 330 Gc indicates the feasibility of this technique. The advantages of oversize waveguide as compared with conventional waveguide and free-space optical components are 1) lower attenuation and 2) simpler construction.**

* Received January 21, 1963. This work was sponsored by Rome Air Development Center, Griffiss Air Force Base, N. Y., under Contract No. AF30(602)-2758.

† Airborne Instruments Laboratory, a Division of Cutler-Hammer, Deer Park, N. Y.

Introduction

THIS PAPER describes the development of components capable of operating at wavelengths below 1 mm. Generally, at frequencies above 300 Gc, components fabricated from conventional single-mode rectangular waveguide are not only excessively lossy (about 10 db per foot) but extremely difficult to construct. In an attempt to overcome this problem, several investigators designed millimeter components (interferometers and directional couplers) using free-space optical techniques. These devices were large structures that had the advantages of somewhat lower attenuation

loss and simplified fabrication. However, the performance of these devices is degraded by diffraction losses. By using rectangular oversize waveguide—that is, waveguide ten times larger than conventional waveguide in each cross-sectional dimension—many of the optical techniques can be applied and insertion loss can be reduced further. This approach is the basis of our research in the submillimeter range.

Oversize Waveguide

A good approximation to plane-wave propagation is obtained in oversize rectangular waveguide (a and b dimensions about ten times greater than standard-size waveguide) if most of the power is contained in the TE_{10} mode.[1] The TE_{10} mode is launched by careful tapering from standard-size waveguide. By operating in this manner, attenuation constants that are lower than standard-size waveguide attenuation constants can be achieved, and the diffraction loss inherent in free-space plane-wave (optical) transmission is also eliminated. In Fig. 1, theoretical attenuation curves for various oversize waveguides are compared with a standard-size waveguide designed for optimum operation at 400 Gc. At 400 Gc, a loss of 7 db per foot for standard-size waveguide reduces to 0.7 db per foot for ten-times oversize waveguide. Although further reductions are possible with still larger waveguides, longer tapers would be required. A loss of 0.7 db per foot is not excessive because most components require path lengths of only 2 or 3 inches. The ten-times oversize waveguide was chosen as a compromise between loss and simplicity of tapering.

Fig. 2 shows the advantage of oversize waveguide over free-space transmission by comparing free-space attenuation with thirty-times oversize waveguide attenuation for a path-length separation of 22.5 cm in the 8.6-mm wavelength range. The results, obtained by Garnham,[1] show that the oversize waveguide loss (curve B) is approximately 0.5 db lower than the free-space loss (curve C). Curve A shows the reference level. Most of the free-space loss can be attributed to diffraction. This loss would not be serious for long-distance transmission techniques such as the Goubau beam waveguide[2] because the diffraction occurs mainly in the launching and receiving horns. It is, however, a distinct disadvantage in components because their path lengths are rarely more than several inches. Oversize waveguide eliminates the launching loss. Waveguide components also have the advantages of being fully shielded and easily transportable; free-space components must be aligned on optical benches.

The main problem created by oversize waveguide is tapering. If a plane wave in the oversize waveguide is launched from a standard-size waveguide, a linear taper at least 50 wavelengths long is required to maintain the same mode pattern as existed in the standard waveguide. This length can be reduced to 5 or 10 wavelengths by using nonlinear tapers,[3,4] Up to the present time, linear tapers have been used because they are easier to fabricate and are of a practicable length in the submillimeter region (6 inches at 300 Gc).

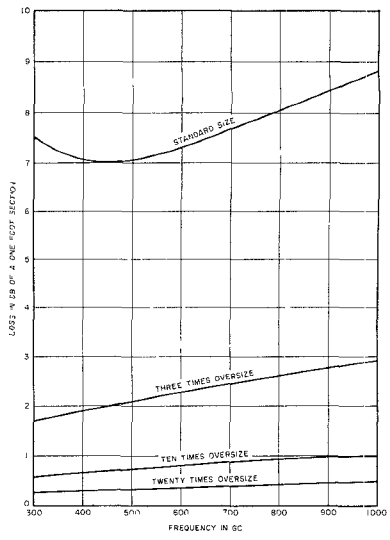

Fig. 1—Comparison of theoretical losses of various size waveguides.

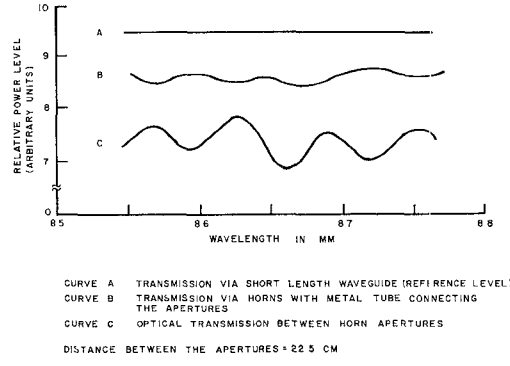

Fig. 2—Comparison of losses of waveguide and free-space transmission lines.

Components

Since oversize waveguide can propagate many undesired modes, it is important to use structures that do not change the modal distribution of the incident wave. Thus, such discontinuities as screws, irises, and slits cannot be used. Optical structures such as prisms, reflectors, and gratings can be used because they operate in a uniform fashion over the entire plane wavefront. A survey of many optical devices that are useful at millimeter and

[1] R. H. Garnham, "Optical and Quasi-Optical Transmission Techniques and Components Systems for Millimeter Wavelengths," Royal Radar Establishment, Malverne, Eng., R.R.E. Rept. No. 3020; March, 1958.

[2] G. Goubau and F. Schwering, "On the guided propagation of electromagnetic wave beam," IRE Trans. on Antennas and Propagation, vol. AP-9, pp. 248–256; May, 1961.

[3] H. G. Unger, "Circular waveguide taper of improved design," *Bell Sys. Tech. J.*, vol. 37, pp. 899–912; July, 1958.

[4] O. Hincklemann, *et al.*, "Second Quarterly Progress Report on New Methods for Measuring Spurious Emissions," Rome Air. Dev. Ctr., N. Y. Rept. No. 1112-1-2, Contract No. AF 30(602)-2511; November, 1961.

submillimeter wavelengths is given in Harvey's paper.[5] We have designed and constructed a directional coupler, a variable attenuator, and a variable phase shifter using the double-prism beam divider.[1,5,6] These components were designed for operation at 345 Gc and used 0.140-inch by 0.280-inch rectangular (ten-times oversize) waveguide. We are presently constructing a circular polarization duplexer and a multiple-slab directional coupler for operation above 300 Gc.

Directional Coupler

The directional coupler consists of two crossed waveguides with a pair of dielectric prisms that are separated by a distance d and placed at the center of the structure [Fig. 3(a)]. A plane-wave incident on the prism from port 1 will be partially reflected to port 2 and partially transmitted to port 3, provided $\sqrt{\epsilon_r}\sin\theta > 1 \cdots$ the total reflection condition. Port 4 is completely decoupled from port 1. The coupling to port 3 is a function of the distance d.

This device has been used successfully in free space in the 8-mm region.[1,6] The design and operation is similar when the device is enclosed in oversize waveguide. The design theory was first derived by Schaeffer and Gross.[7] Their theory indicates that a pair of matched lossless prisms operating on an electric field that is polarized perpendicular to the plane of incidence will split the input power between ports 2 and 3 as follows:

$$\frac{P_2}{P_1} = \frac{(\epsilon_r - 1)^2 \sinh^2 \alpha d}{\sinh^2 \alpha d + \epsilon_r(\epsilon_r - 2)\cosh^2 \alpha d} \tag{1}$$

and

$$\frac{P_3}{P_1} = \frac{\epsilon_r(\epsilon_r - 2)}{\sinh^2 \alpha d + \epsilon_r(\epsilon_r - 2)\cosh^2 \alpha d} \tag{2}$$

where

$$\alpha = \frac{2\pi}{\lambda}\sqrt{\epsilon_r/2 - 1}.$$

A plot of P_3/P_1 vs d/λ is given in Fig. 4 for various dielectric constants. These curves were used to design the variable directional coupler, shown in Fig. 3, using Rexolite (ϵ_r estimated to be 2.55). For example, a 10-db coupler requires $d/\lambda = 0.5$ or $d = 0.0197$ inch at 300 Gc. The prism surfaces must be matched to the four ports if the shapes of the experimental power ratio curves are

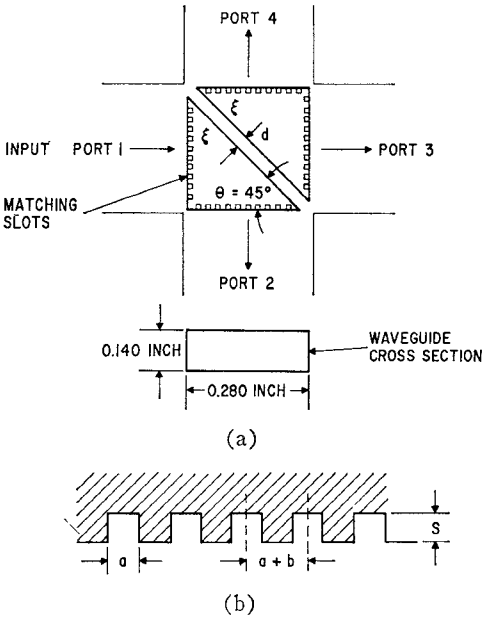

Fig. 3—Double-prism directional coupler. (a) Structure. (b) Slot dimensions.

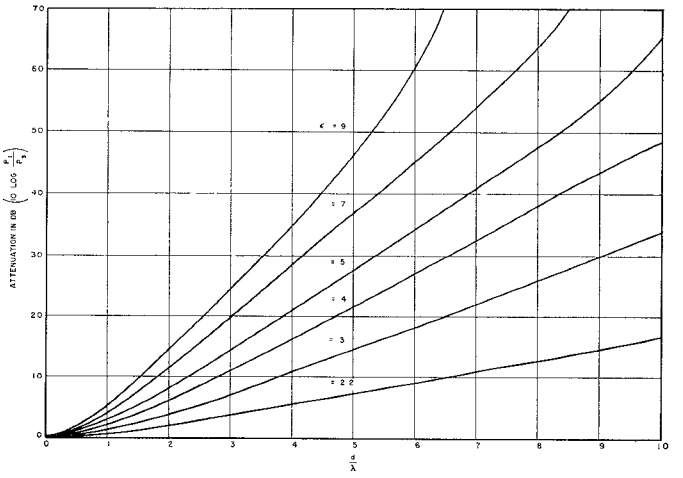

Fig. 4—Attenuation of double-prism device.

to agree with those predicted by (1) and (2). Matched prisms were obtained by slotting the surfaces facing the four ports [Fig. 3(b)] using design equations given by Garnham.[1] The results at 345 Gc using Rexolite prisms are [Fig. 3(b)]:

$$a = 0.0022 \text{ inch}$$
$$a + b = 0.008 \text{ inch}$$
$$s = 0.0067 \text{ inch}.$$

These slots were cut parallel to the direction of the polarization of the electric field. Fig. 5 is a photograph of a slotted Rexolite prism designed for operation at 345 Gc. We have not as yet evaluated the matching effectiveness at this frequency but, based on experience in the 8-mm wavelength region, we expected to obtain surface voltage-reflection coefficients of less than 0.02.

[5] A. F. Harvey, "Optical techniques at microwave frequencies," *Proc. IEE*, Paper No. 2799E, p. 154; March, 1959.
[6] R. G. Fellers, "Applications of Dielectric Prisms at Millimeter Wavelengths," Dept. Elec. Eng., University of South Carolina, Columbia, AD-219785; July, 1959.
[7] C. Schaefer and G. Gross, "Investigations concerning total reflection," *Ann. der Phys.*, vol. 32, p. 648, 1910.

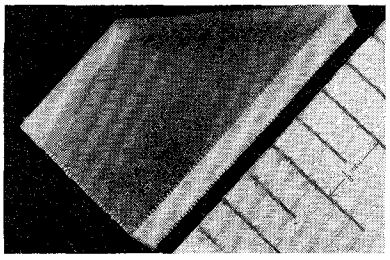

Fig. 5—Slotted prism.

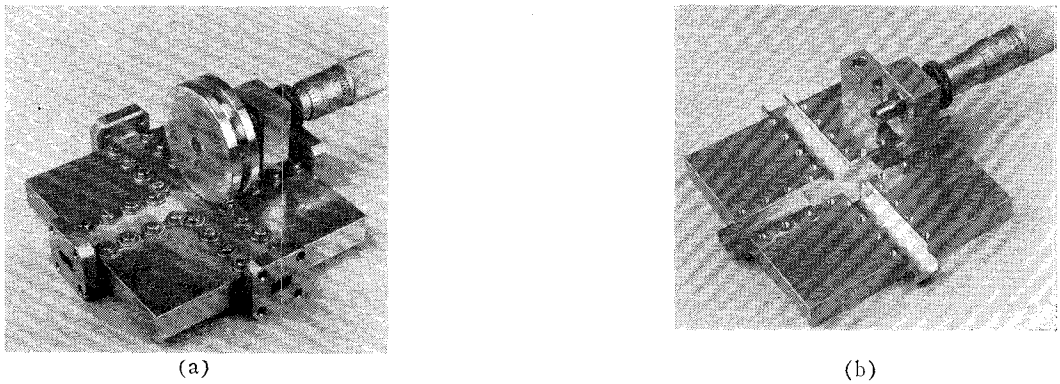

(a) (b)

Fig. 6—Ten-times oversize directional coupler. (a) Assembled. (b) Disassembled.

Losses in the double prism can be estimated as the sum of the dielectric and the wall attenuation. The dielectric attenuation in a highly oversize waveguide is

$$\alpha = \frac{\sqrt{\epsilon_r}\, 692 \tan \delta}{\lambda} \text{ db/inch} \tag{3}$$

where

λ = free-space wavelength in millimeters
ϵ_r = real part of the relative complex dielectric constant
$\tan \delta$ = dielectric loss tangent.

There is no data available on loss tangents in the submillimeter region at this time. An extrapolation of 140-Gc data obtained from Cohn *et al.*,[8] gives a tan δ of 0.0023 for Rexolite. Using this value at a wavelength of 1 mm and assuming that $\epsilon_r = 2.55$ gives an α of 2.6 db/inch. The maximum dielectric path length is 0.5 inch in the double-prism coupler, which yields an estimated dielectric loss of 1.3 db. The wall losses are estimated by using the curve for ten-times oversize waveguide shown in Fig. 1 (0.6 db per foot at 300 Gc.) The total path length from the input port to any coupled port is about 4 inches, thereby giving an estimated loss of 0.24 db. Adding this wall loss to the dielectric loss gives a total estimated dissipation loss of 1.54 db.

[8] M. Cohn, F. Sobel, and J. Cotton, "Millimeter Wave Research," Rome Air Dev. Ctr., N. Y., Tech. Note No. 1, Contract No. AF 30(602)-2457; November, 1961.

Photographs of the assembled and disassembled directional coupler are shown in Fig. 6. The separation of the prisms is adjusted by a micrometer-driven wheel that is connected to one of the prisms by a Rexolite tab projecting from the prism closest to the micrometer [Fig. 6(b)]. The other prism is stationary. The crossed waveguide is constructed from a three-sided brass waveguide with a top wall bolted into position. The surface finish on the waveguide walls is less than five microinches. This device can be adjusted for any desired coupling ratio by adjusting the micrometer.

Variable Attenuator

The double-prism coupler is a variable attenuator when ports 2 and 4 are terminated in matched loads (Fig. 3). We have used open-ended oversize waveguides as terminations; their SWR's are under 1.1. The variation of attenuation with prism separation is given by (2). The attenuation, expressed in db, is

$$A = 10 \log \frac{P_1}{P_3} = 10 \log \left[1 + \frac{(\epsilon_r - 1)^2}{\epsilon_r(\epsilon_r - 2)} \sinh^2 \alpha d \right] \text{db} \tag{4}$$

which for large $\alpha d (\alpha d > 2)$ becomes

$$A \approx 20 \log \left[\frac{(\epsilon_r - 1)}{2\sqrt{\epsilon_r(\epsilon_r - 2)}} \right] + 8.68 \alpha d \text{ db}. \tag{5}$$

The attenuation should therefore approach a linear function of d for large αd.

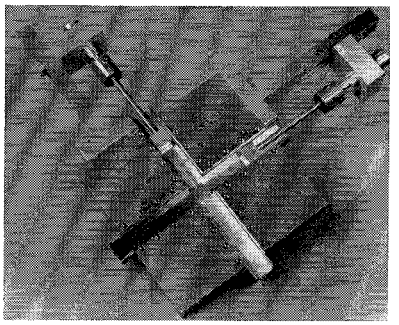

Fig. 7—Phase shifter.

Eq. (5) illustrates the usefulness of this device as a simple attenuation standard. Furthermore, the quantity α can be obtained from measurements of the slope of the attenuation vs distance curve and, therefore, is a means of accurately obtaining ϵ_r.

The attenuator was matched in exactly the same way as the coupler—a series of slots were machined on the four surfaces of the prism.

Phase Shifter

A 300-Gc variable phase shifter was constructed by choosing a distance d for the double-prism structure that corresponds to 3-db coupling and placing ganged sliding shorts on ports 2 and 3. Fig. 7 shows the construction of this device. The operating principle of this device is identical to that of a phase shifter formed by inserting a pair of sliding shorts into two arms of a short-slot hybrid junction. The shorts consist of brass blocks with a 0.002-inch layer of Teflon bonded to the periphery. The final unit will be gold-flashed. The shorts are moved by vernier micrometer heads. The position of the shorts can be set to within 0.0001 inch. Since a 0.020-inch movement corresponds to a phase shift of 360 degrees at 300 Gc, a deviation of 0.0001 inch corresponds to a 1.8-degree error. Since the operation of this device depends on good surface matching, the previously discussed prism slotting technique was also used in this component.

Multiple-Slab Coupler

Another type of variable directional coupler and attenuator is shown in Fig. 8. It consists of two or more dielectric slabs placed on both sides of the centerline at 45 degrees to the direction of incident power flow. Each slab has a thickness t yielding an electrical length of 90 degrees and is separated by d_1—a quarter-wavelength section of air. The coupling is varied by adjusting d_2. An analysis of this device is given in Appendixes I and II for the one- and two-slab cases respectively. The characteristics of the one- and two-slab cases are shown in Figs. 9 and 10.

At the present time, a three-slab coupler designed for operation at 330 Gc is being fabricated using quartz slabs in oversize waveguide.

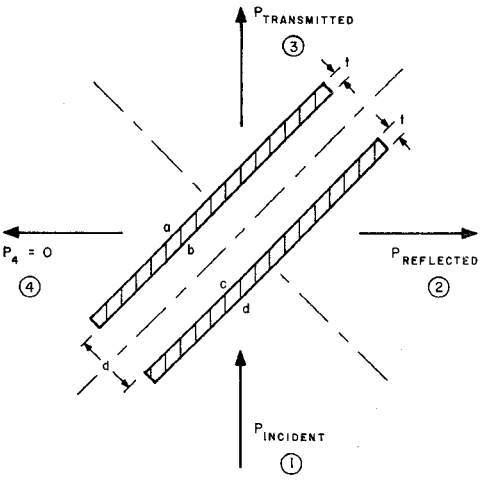

(a)

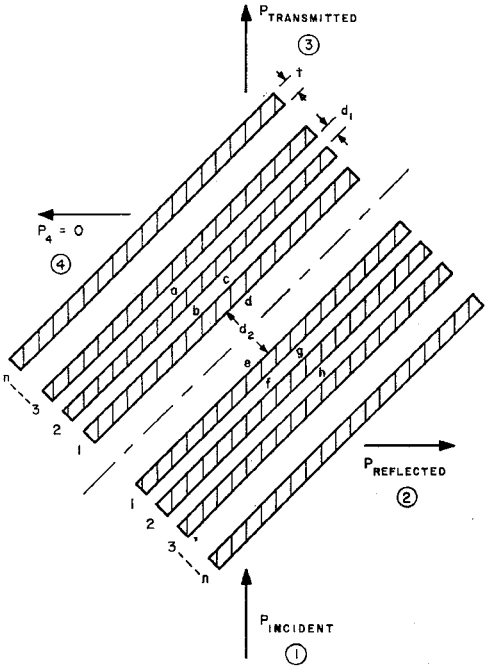

(b)

Fig. 8—Multiple-slab coupler. (a) Pair of single-dielectric slabs. (b) Pair of multiple-dielectric slabs.

Experiments With Oversize Waveguide Components

The first experiments were performed on a double-prism coupler operating at a center frequency of 3 Gc using three-times oversize waveguide; successful operation was obtained. The results of these experiments are given by Hindin and Taub.[9] A ten-times oversize

[9] H. Hindin and J. J. Taub, "Oversize waveguide directional coupler," IRE Trans. on Microwave Theory and Techniques (*Correspondence*), vol. MTT-10, pp. 394–395; September, 1962.

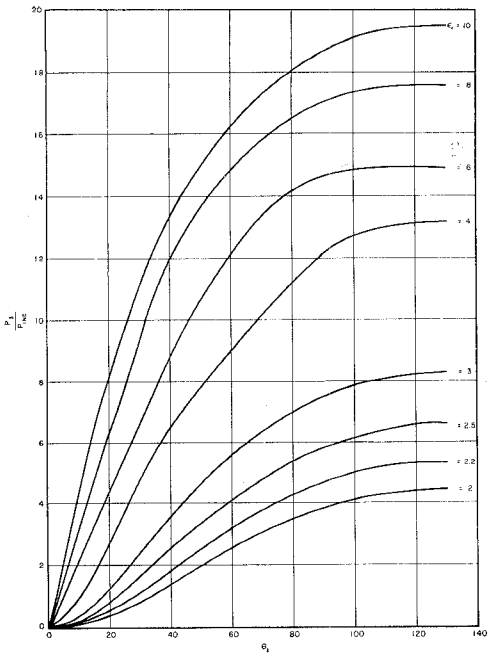

Fig. 9—Attenuation of $N=1$ multiple-slab coupler.

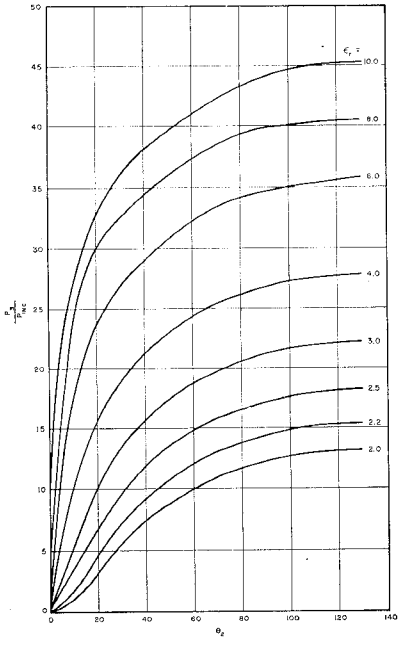

Fig. 10—Attenuation of $N=2$ multiple-slab coupler.

double-prism coupler was then designed for 10-db coupling at a center frequency of 27 Gc. This device used standard S-band waveguide, and the Rexolite prisms were surface-matched by means of quarter-wavelength slabs of Eccofoam chosen for $\epsilon_r = 1.6$. The experimental results are shown in Fig. 11.

The directivity was greater than 30 db over a narrow band and the desired 10-db coupling was obtained within 0.5 db. These results proved the feasibility of the ten-times oversize waveguide and enabled us to construct our submillimeter device by carefully scaling the oversize device.

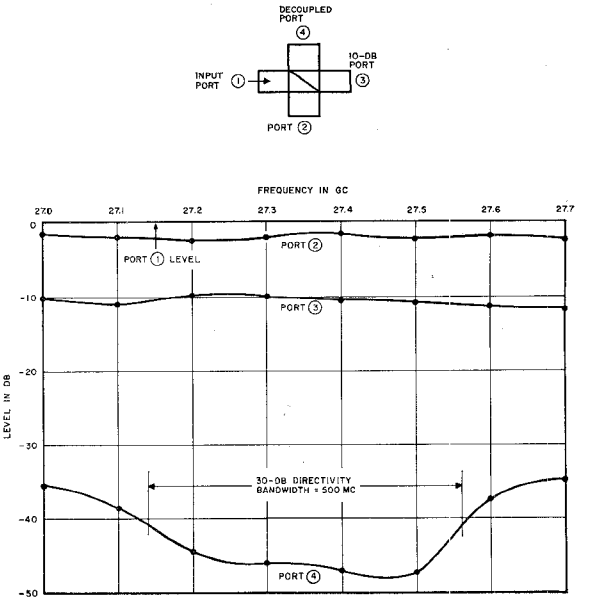

Fig. 11—Measured characteristics of 27-Gc double-prism coupler.

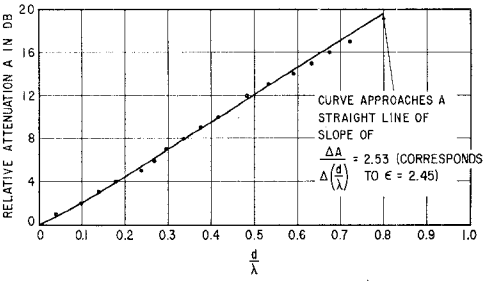

Fig. 12—Attenuation vs distance between Rexolite prisms at 330 Gc.

A movable double-prism device was given a preliminary evaluation as a variable attenuator and directional coupler at 330 Gc. The prism surfaces were not slotted; this caused a slight ripple in the attenuation vs d/λ curve. Nevertheless, a plot of measured attenuation vs d/λ approached a straight line as predicted (Fig. 12). The slope of this line corresponds to an ϵ_r of 2.45. The slight deviations of the measured points from a smooth curve are attributed to the interface matching. A single measurement of power coupled to port 4 showed a directivity of at least 10 db; a limited signal-to-noise ratio prevented a more exact determination. These results suggest that a directivity greater than 20 db can be expected if a pair of surface-matched prisms are used.

The 330-Gc measurements were made with a CSF carcinotron at Lincoln Laboratory. The carcinotron output was fed to a 0.011-inch by 0.022-inch squeeze section to filter any modes other than TE_{10}. This squeeze section was followed by a series of tapers to the oversize waveguide. The power was detected using a bolometer followed by a tuned 1000-cps amplifier. The carcinotron was modulated by means of a ferrite modulator constructed in 90- to 140-Gc waveguide. The tapers and squeeze section are shown in Fig. 13.

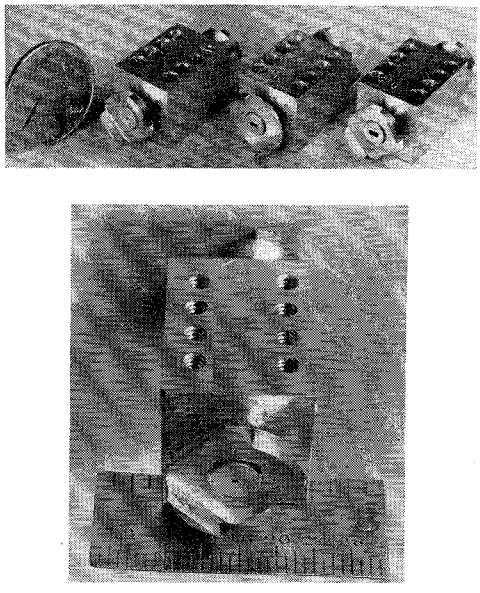

Fig. 13—Tapers and squeeze section (0.011 by 0.022 inch).

Conclusions

Preliminary measurements indicate oversize quasi-optical waveguide is feasible for directional couplers, attenuators, and phase shifters in the submillimeter as well as the millimeter wavelength region. Work is continuing on duplexers and couplers using multiple dielectric slabs. Components designed using this technique should have lower attenuation values and should be easier to fabricate than conventional rectangular waveguide. In addition, they will have lower insertion loss, be inherently shielded, and be more easily transportable than free-space optical components.

Appendix I

Reflection and Transmission Properties of a Pair of Movable Dielectric Slabs

This Appendix derives the properties of a movable dielectric slab structure [Fig. 8(a)]. The slabs have relative dielectric constants (ϵ_r), are assumed to be lossless, and have a thickness t equal to 90 electrical degrees. The object of this analysis is to obtain the reflection and transmission coefficients as a function of the slab separation d_1. The impedance at plane b for a 90-degree dielectric slab is

$$Z_b = \frac{Z_\epsilon^2}{Z_a} \tag{6}$$

where

Z_a = characteristic impedance in air for a direction 45 degrees from the vertical—$120\pi\sqrt{2}$

Z_ϵ = characteristic impedance in the dielectric for a wavelength that is traveling in a direction of 45 degrees at the air interface—$Z_\epsilon = 120\pi \sec\theta_2/\sqrt{\epsilon_r}$, where, from Snell's law,

$$\sin\theta_2 = \frac{\sin 45 \text{ degrees}}{\sqrt{\epsilon_r}};$$

Z_ϵ reduces to

$$120\pi\sqrt{\frac{2}{2\epsilon_r - 1}}.$$

The impedance at plane c is obtained from transmission-line theory

$$Z_c = \left[\frac{Z_b + jZ_a \tan\dfrac{2\pi d_1}{\sqrt{2}\,\lambda}}{Z_a + jZ_b \tan\dfrac{2\pi d_1}{\sqrt{2}\,\lambda}}\right] \tag{7}$$

which in turn gives

$$Z_d = \frac{Z_\epsilon^2}{Z_c} = \frac{120\pi\sqrt{2}\left[Z_a + jZ_b \tan\dfrac{2\pi d_1}{\sqrt{2}\,\lambda}\right]}{(2\epsilon_r - 1)\left[Z_b + jZ_a \tan\dfrac{2\pi d_1}{\sqrt{2}\,\lambda}\right]}. \tag{8}$$

The reflection coefficient at plane d can be obtained from (8),

$$\Gamma_d = \frac{Z_d - Z_a}{Z_d + Z_a} = \frac{j \tan\dfrac{2\pi d_1}{\sqrt{2}\,\lambda}\left[\dfrac{1}{(2\epsilon_r - 1)^2} - 1\right]}{j \tan\dfrac{2\pi d_1}{\sqrt{2}\,\lambda}\left[\dfrac{1}{(2\epsilon_r - 1)^2} + 1\right] + \dfrac{2}{2\epsilon_r - 1}}. \tag{9}$$

The power coupled to port No. 2 in Fig. 8(a) is $|\Gamma_d|^2 P_1$. From (9), $|\Gamma|^2$ is

$$\frac{P_2}{P_1} = |\Gamma_d|^2 = \frac{\tan^2 0.707\theta_1\left[\dfrac{1}{(2\epsilon_r - 1)^2} - 1\right]^2}{\dfrac{4}{(2\epsilon_r - 1)^2} + \tan^2 0.707\theta_1\left[\dfrac{1}{(2\epsilon_r - 1)^2} + 1\right]^2} \tag{10}$$

where

$$\theta_1 = \frac{2\pi d_1}{\lambda}.$$

For lossless slabs, the power coupled to port No. 3 in Fig. 8(a) is $(1 - |\Gamma_d|^2)P_1$. Therefore,

$$\frac{P_3}{P_1} = 1 - |\Gamma_d|^2 = \frac{\dfrac{4}{(2\epsilon_r - 1)^2}\sec^2 0.707\theta_1}{\dfrac{4}{(2\epsilon_r - 1)^2} + \tan^2 0.707\theta_1\left[\dfrac{1}{(2\epsilon_r - 1)^2} + 1\right]^2}. \tag{11}$$

Appendix II

Reflection and Transmission Properties of a Pair of Movable Double Slabs

This Appendix derives the reflection and transmission coefficients of the double-slab structure shown in Fig. 8(b) (slabs 3 through n are not considered). The impedance at plane d is obtained from (8). In this structure, $2\pi d_1/\sqrt{2}\lambda$ is chosen to be $\pi/2$. This gives a Z_d of

$$Z_d = \frac{120\pi Z_b\sqrt{2}}{(2\epsilon_r - 1)Z_a} = \frac{120\pi\sqrt{2}}{(2\epsilon_r - 1)^2}. \tag{12}$$

The value of Z_e can now be obtained,

$$Z_e = Z_a\left[\frac{Z_d + jZ_a\tan\dfrac{2\pi d_2}{\sqrt{2}\lambda}}{Z_a + jZ_d\tan\dfrac{2\pi d_2}{\sqrt{2}\lambda}}\right]. \tag{13}$$

This is transformed through a quarter-wavelength section of Z_e,

$$Z_f = \frac{(Z_e)^2}{Z_e}. \tag{14}$$

Similarly,

$$Z_g = \frac{(Z_a)^2}{Z_f} \quad \text{and} \quad Z_h = \frac{(Z_e)^2}{Z_g}. \tag{15}$$

Using (13)–(15)

$$Z_h = Z_a\left(\frac{Z_g}{Z_a}\right)^4\left[\frac{1 + j\dfrac{Z_d}{Z_a}\tan\dfrac{2\pi d_2}{\sqrt{2}\lambda}}{\dfrac{Z_d}{Z_a} + j\tan\dfrac{2\pi d_2}{\sqrt{2}\lambda}}\right] \tag{16}$$

which reduces to

$$Z_h = 120\pi\sqrt{2}\left(\frac{1}{2\epsilon_r - 1}\right)^2 \cdot \left[\frac{\dfrac{\tan\dfrac{2\pi d_2}{\sqrt{2}\lambda}}{1 + j\dfrac{}{(2\epsilon_r - 1)^2}}}{\dfrac{1}{(2\epsilon_r - 1)^2} + j\tan\dfrac{2\pi d}{\sqrt{2}\lambda}}\right]. \tag{17}$$

The reflection coefficient at plane h is

$$\Gamma_h = \frac{Z_h - Z_a}{Z_h + Z_a} = \frac{j\tan\dfrac{2\pi d_2}{\sqrt{2}\lambda}\left[\dfrac{1}{(2\epsilon_r - 1)^4} - 1\right]}{\dfrac{2}{(2\epsilon_r - 1)^2} + j\tan\dfrac{2\pi d}{\sqrt{2}\lambda}\left[\dfrac{1}{(2\epsilon_r - 1)^4} + 1\right]}. \tag{18}$$

Finally, the power reflection coefficient $|\Gamma_h|^2$ is

$$|\Gamma_h|^2 = \frac{\tan^2 0.707\theta_2\left[\left(\dfrac{1}{2\epsilon_r - 1}\right)^4 - 1\right]^2}{4\left(\dfrac{1}{2\epsilon_r - 1}\right)^4 + \tan^2(0.707\theta_2)\left[\left(\dfrac{1}{2\epsilon_r - 1}\right)^4 + 1\right]^2} \tag{19}$$

where

$$\theta_2 = \frac{2\pi d_2}{\lambda}$$

and the power transmission coefficient $1 - |\Gamma_h|^2$ is

$$\frac{P_3}{P_1} = 1 - |\Gamma_h|^2 = \frac{4\left(\dfrac{1}{2\epsilon_r - 1}\right)^4\sec^2(0.707\theta_2)}{4\left(\dfrac{1}{2\epsilon_r - 1}\right)^4 + \tan^2(0.707\theta_2)\left[\dfrac{1}{(2\epsilon_r - 1)^4} + 1\right]^2}. \tag{20}$$

Acknowledgment

The authors wish to express their appreciation to B. F. Thaxter, P. Tannenwald, and G. Heller of M.I.T. Lincoln Laboratory, Lexington, Mass., for making their 1-mm carcinotron available for evaluating the oversize waveguide components.